POLITECNICO DI TORINO
Repository ISTITUZIONALE

High-Temperature Annealed Biochar as a Conductive Filler for the Production of Piezoresistive Materials for Energy Conversion Application

(Article begins on next page)

20 March 2024

Article

High-Temperature Annealed Biochar as a Conductive Filler for the Production of Piezoresistive Materials for Energy Conversion Application

Mauro Giorcelli,* Mattia Bartoli, Alessandro Sanginario, Elisa Padovano, Carlo Rosso, Massimo Rovere, and Alberto Tagliaferro

Cite This: https://dx.doi.org/10.1021/acsaelm.0c00971

Read Online

ACCESS | Metrics & More | Article Recommendations | Supporting Information

ABSTRACT: In this research work, we develop a prototype that is able to convert mechanical strain into an electrical signal. To reach this scope, we evaluated the electrical properties of a thermally annealed biochar-based silicon composite. The great elasticity range of silicon will provide the mechanical properties for the realization of an effective piezoresistive material. For the fulfillment of this aim, we annealed olive biochar at 1500 °C in order to achieve a good degree of graphitization and an electrical conductivity close to 10^3 S/m. The electrical conductivity under the mechanical stress of composites was deeply investigated through experiments and simulation to achieve a comprehensive knowledge. Furthermore, a real device based on these composites was designed and realized to demonstrate one of the prospective exploitations of the composite piezoresistive properties.
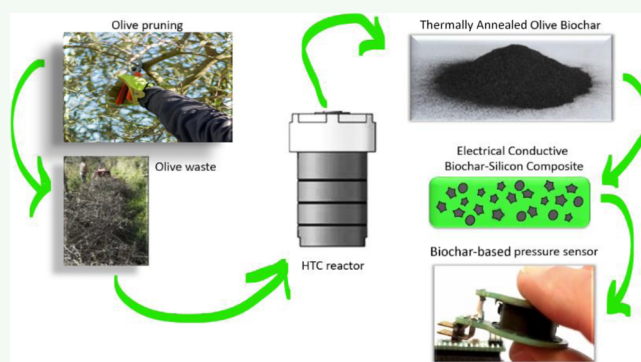
1. INTRODUCTION

During the last decades, biochar has attracted the interest of the scientific community not only for soil and fuel applications[1,2] but also as a carbonaceous source for high value-added cost applications. By combining the low cost and a reduced environmental footprint, biochar is a strong candidate to become the carbon source for a new era of materials science.[3] Since the pioneering works of Das and co-workers,[4,5] biochar has proven itself an extremely sound choice for toughening a wide range of both the thermoset and thermoplastic polymeric matrix.[6−11] Furthermore, Khan et al.[12,13] used biochar as a replacement for traditional high-performance carbon fillers such as CNTs reaching better mechanical performances. Nonetheless, the electrical properties of biochar are far from reaching the outstanding properties of graphene and CNTs mainly due to the small size and poor quality of the graphitic domains.[14,15] Graphitization of biochar can be improved by pyrolyzing it at temperatures exceeding 800 °C[16−19] or through postproduction thermal annealing at a temperature close or above 900 °C.[20−22] This productive way is easier to manage due to the limited production of the volatile organic matter during early stages of pyrolysis. Furthermore, higher temperatures could be reached by using the postproduction annealing process due to the possibility of using sintering ovens instead of pyrolytic units. The use of

temperature up to 1000 °C leads to a dramatic increase in electrical conductivity due to the formation and reorganization through turbostratic rearrangement[23] of the graphitic domains as described by Eom et al.[24]

The highly conductive biochar obtained after the graphitization treatment represents a very attractive filler for the realization of plenty of electrically conductive composites. Its high dispersibility together with the improved properties enhanced the range of application far beyond those merely exploiting the mechanical improvement. One of the most interesting new fields of application could be represented by the development of reversible piezoresistive composites.[25] Nowadays, only one study is reported in the literature about the use of biochar for this specific task by Nan et al.[26] However, the authors studied a poly(vinyl alcohol)-based system that can grant good piezoresistive response and reversibility but dramatically lacks in chemical resistance. To tackle this issue while keeping a good piezoresistive response,

we used a silicon rubber. Silicon rubbers are very resistant to harsh chemical environments,[27] allowing the production of more resistant composites. By adding thermally annealed olive biochar (TAOB), we developed a piezoresistive material. Herein, we report a comprehensive study on TAOB−silicon composite piezoresistive properties by both experimental and computational approaches. Furthermore, we realized an electronic device based on TAOB composites that is able to convert a mechanical deformation (pressure) into an electrical signal.

2. MATERIALS AND METHODS

2.1. Materials. Olive wastes were collected and dried at 105 °C for 72 h in a ventilated oven. A detailed characterization of the feedstock was reported elsewhere by Bartoli et al.[18]

Bicomponent silicon rubber (GLS-50) was purchased from Prochimica Italia and used without further modifications. The electronic controller used in this work is called "Arduino Micro", and it is a microcontroller board based on ATmega32U4. Arduino is a computer hardware and software company, project and open-source consumer community that designs and manufactures single micro-controllers and microcontroller kits to build digital devices. It was purchased by RS Components S.r.l. The top and bottom electrodes for the TAOB composite are custom printed circuit boards (PCBs) designed by the authors.

2.2. Methods. Olive wastes were cut into cylindrical pieces (diameter 3 cm, length 15 cm) and pyrolyzed in a tubular furnace (Carbolite TZF 12/65/550) in a nitrogen atmosphere at 15 °C/min and kept at the highest treatment temperature of 400 °C for 30 min and cooled down. Afterward, they were mechanically ground for 10 min.

Grinded biochar was annealed by using a vacuum electric furnace (Pro.Ba., Cambiano, Italy) under an argon atmosphere (99.99% purity, controlled pressure 550 mbar) using a heating rate of 150 °C/ h, a dwell at a maximum temperature of 1500 °C for 30 min, and a cooling to room temperature with the same thermal gradient used for heating. Afterward, TAOB was mechanically pulverized to reduce the particle size in the micrometer range. TAOB particle size distribution was evaluated using laser granulometry (Fritsch Analysette 22, Idar-Oberstein, Germany) after dispersion in ethanol and sonication in an ultrasonic bath for 10 min. The morphology of TAOB and related composites was investigated using field-emission scanning electron microscopy (FE-SEM, Zeis Supra 40). Raman spectra were collected using a Renishaw inVia (H43662 model, Gloucestershire, UK) equipped with a green laser line (514 nm) with a 50× objective. Raman spectra were recorded in the range from 250 to 3500 cm^{-1}. TAOB-based silicon composites were produced by mechanically mixing TAOB particles with silicon prepolymers and after the catalyst was added. The mixture was left in a polycarbonate mold at room temperature for 16 h until the completion of polymerization. TAOB-based composites were produced in a cylindrical shape and tested by using an MTS machine (MTS Q-test10).

Vigorous mixing procedures lead to an uncontrollable decrement of the biochar particle size.[8,16−18,28,29] Hence, TAOB-based composites were prepared by gently mechanical mixing TAOB with a silicon-based prepolymer for 3 min. Afterward, tin octoate was added as the catalyst for the polymerization and mixed again for other 3 min. Samples were left overnight at room temperature in poly(carbonate) molds until the completion of the polymerization process.

Biochar and related composite conductivity were estimated by a modification of the setup proposed by Gabhi et al.[30] and reported by Giorcelli and Bartoli.[17,20]

2.2.1. Demonstration Board. In order to realize a portable and low-cost application demo, a commercial NeoPixel RGB 5050 light-emitting diode (LED) was utilized as a visual indicator with its color varying following the force applied on the biochar pressure sensor. In this way, for increasing the load applied on the sensor, the LED light

color would range from green (low mechanical force) to red (high mechanical force) passing by yellow, as summarized in Figure 1.
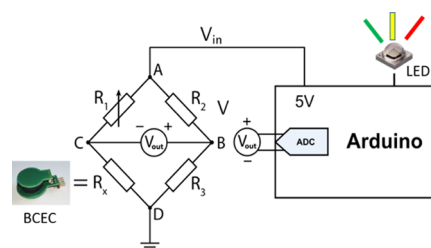

Figure 1. Scheme of the device based on TAOB composites. The two V_{out} are both measured between B and C. We replicated the label to avoid burdening the figure with too many lines.

In our setup, the R_x of Figure 1 is represented by the piezoresistive button [biochar composite energy converter (BCEC)] and the Wheatstone bridge is balanced (i.e., $V_{BC} = V_{out} = 0$) before applying force to the button by adjusting the value of the resistor R_1. This occurs when

$$\frac{R_1}{R_{0x}} = \frac{R_2}{R_3}$$

where R_{0x} is the resistance of the button with no pressure applied. Once this step is performed, applying a force to the button, thus causing a variation of its R_x value, will lead to an unbalanced bridge situation (i.e., $V_{BC} = V_{out} \neq 0$). In such a situation, assuming that no currents flow in the BC branch, the voltage V_{out} will be given by

$$V_{out} = \left(\frac{R_x}{R_x + R_1} - \frac{R_3}{R_3 + R_2} \right) V_{in}$$

As the V_{in} value is kept constant (= 5 V), the variation in the V_{out} value will solely be due to the variation of the piezoresistive button resistance. As the procedure requires the Wheatstone bridge to be initially balanced, the set of bridge resistors for each demo board was carefully selected on the basis of the unloaded button resistance R_{0x}. In future, digital potentiometers will be used in order to easily accommodate the device to the different unloaded button resistances. To create a stable and firm contact between the biochar composite and the two electrodes, we developed two PCBs. The production procedure is shown in Figure 2.

First, we prepared the blend of silicon and TAOB [Figure 2] and we uniformly distributed it on one of the two electrodes [Figure 2]. Here, we confined it by using a poly(carbonate) ring and we applied the other electrode on top of the blend leaving the system under moderate pressure for the polymerization process [Figure 2]. After 16 h, we removed the poly(carbonate) ring and we obtained a complete silicon/TAOB BCEC [Figure 2]. The final step is the addition of a 90° male header [Figure 2] to interface the BCEC with the signal conditioning board. The final demo board is shown in Figure 3; it is an interfacing PCB for an Arduino Micro containing a DC/DC boost converter to raise 3 V, coming from a coin-cell lithium battery, to 5 V necessary to power up Arduino itself. Such 5V is used to feed the Wheatstone bridge and the RGB LED as well. A simple 90° female header connector is placed on the edge of the PCB to connect the biochar pressure sensor.

The algorithm coded in the firmware was kept basic to save power in the perspective of a portable device. At the startup, the system measured the input of BCEC and set such values as the baseline. As the key was increasingly pressed, its resistance decreased, with the LED color changing smoothly from green to red passing by yellow. The maximum pressure, corresponding to a full red color, was set by one-time-only manually pressing the key with the highest compression we could reach with our fingers. In this way, with a fixed top level, and by reading the base level every time, the system was able to dynamically normalize the color scale to every new startup.
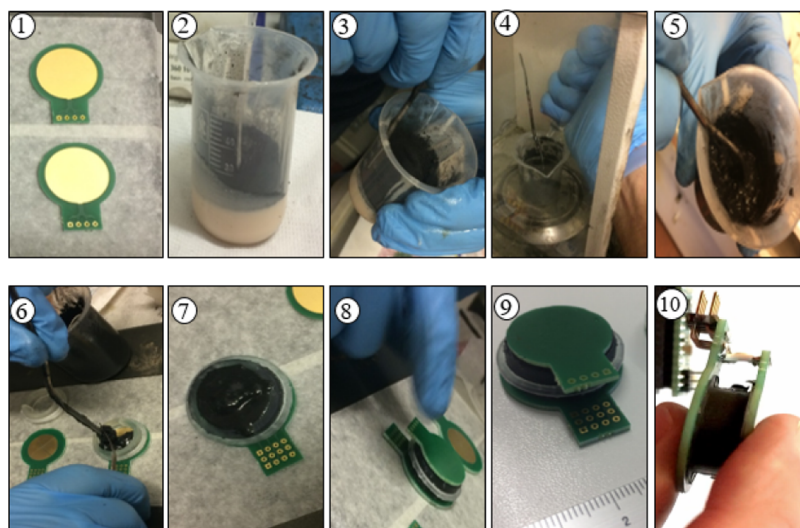
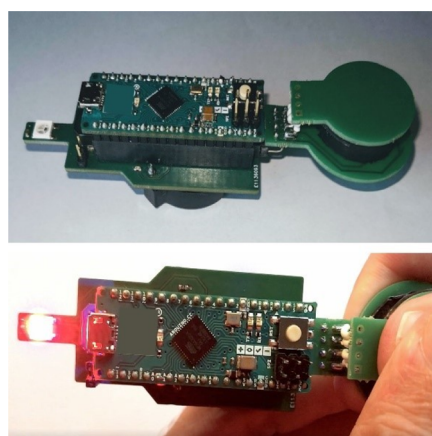**Figure 2.** Production procedure of the electrode PCB based on TAOB composites.

Figure 3. Demo device. Up, the silicon pressure sensor; down, the LED indicator.

2.3. Compression Modeling.

The modeling of the electrical conductivity variation under compression was developed exploiting the software described by Castellino et al.[31] and implemented by using a homemade software compiled using Matlab and a Dijkstra algorithm.[32] The method aimed to find the least electrically resistive path between two flat electrodes. The space between the electrodes is filled with the composite and is reduced as the pressure is increased, taking into account the elastic modulus of the composite. In the computation, we assume that TAOB particles gave a null contribution to the resistance due to their high conductivity ($\sigma > 10^3$ S/m) with respect to that of the host polymer ($\sigma < 10^{10}$ S/m). As a consequence, the least resistive (i.e., the most conductive) paths are those having the shortest length traveled inside the polymer. Our software singles out such paths among all possible paths between the electrodes. We decided to work with a 3D cubic cell with an edge length of 0.5 mm and with randomly distributed spherical impenetrable particles with sizes ranging from 50 to 100 μm modeling a composite containing around 25 wt % of TAOB, the same concentration used for the device realization mentioned above. We assumed that Poisson's module is low enough to avoid any significant deformation of the composite in the device in the range of explored pressure.

3. RESULTS

3.1. Biochar and TAOB Preliminary Characterization.

Pristine biochar produced at 400 °C and TAOB were first

characterized through morphological analysis by using FESEM, as shown in Figure 4.

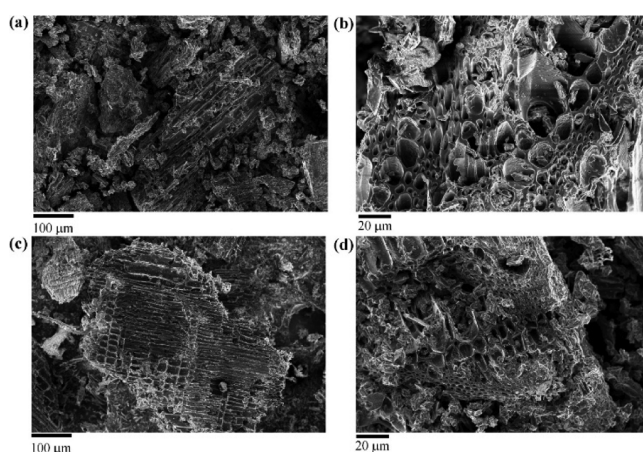**Figure 4.** FESEM captions at different magnifications of (a,b) biochar produced at 400 °C and (c,d) TAOB.

Biochar produced at 400 °C showed a remarkable retention of the original wood structure with xylem and phloem tissues clearly visible after carbonization (Figure 4b). This extended channeled structure was also preserved in TAOB (Figure 4d). Furthermore, the particle size of olive maintained a similar size, as shown in Figure 4a,c with big-sized particles. Nonetheless, FESEM is a merely qualitative analysis and cannot provide a trustworthy particle size distribution, while these characteristics play a key role in the conduction phenomena of composites as reported by Jing et al.[33] Therefore, we analyzed particle size distribution through scattering techniques obtained from the profile shown in Figure 5.

TAOB particle distribution showed two main peaks centered, respectively, close to 25 and 100 μm with few bigger particles in the submillimetric range. Afterward, we estimated the conductivity of TAOB according to the methodology reported by Giorcelli et al.[12] and compared it with that of the olive biochar produced at 400 °C. Results clearly enlighten the increase in conductivity due to the thermal annealing that leads to an olive biochar conductivity exceeding 10^3 S/m for TAOB.
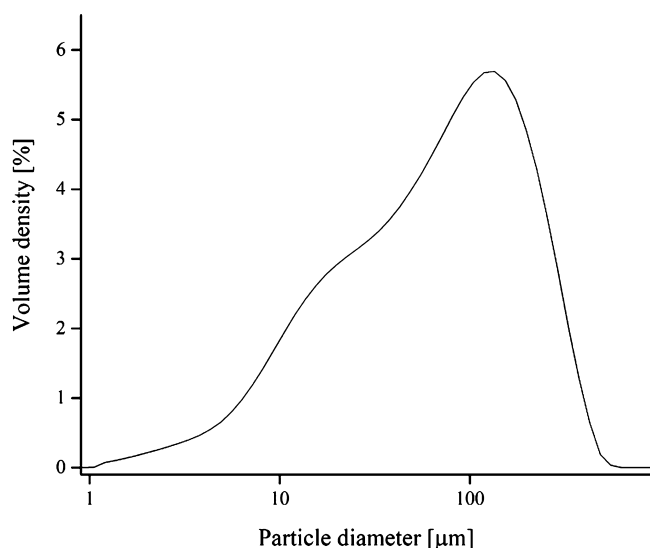
C

Figure 5. Particle size distribution of TAOB.

This is mainly due to the high graphitization that occurred to the material during the treatment at 1500 °C as witnessed by the Raman spectra reported in Figure 6.
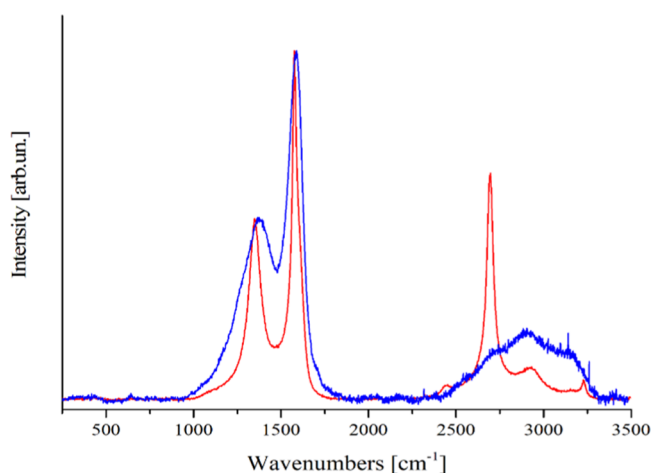

Figure 6. Raman spectra of biochar produced at 400 °C (blue line) and TAOB (red line).

The evolution of biochar structures due to the increase in treatment temperature could be monitored through Raman spectroscopy according to Ferrari et al.[34] Olive biochar showed a large D peak centered at 1380 cm^{-1} and a D peak centered at 1588 cm^{-1}. The peak position together with the bumped poor-defined second-order Raman peaks in the range between 2500 and 3100 cm^{-1} identified this material as a carbon still rich in sp^3 with a low order in aromatic domains that were just starting to form. TAOB showed a very different spectrum with a much more structured second-order Raman region. Furthermore, both D and G peaks were narrower and showed a more pronounced dip between them. Considering TAOB, the D peak was centered at 1350 cm^{-1}, while the G peak was centered at 1575 cm^{-1}, suggesting a carbonaceous material composed by nanographitic domains with a negligible amount of sp^3 sites. The high graphitic structure of TAOB is accountable for the high conductivity observed.[35,36]

3.2. TAOB Composite Characterization.

TAOB was mixed with a silicon rubber for the production of composites with a filler percentage ranging from 15 up to 30 wt %. A preliminary characterization of TAOB-based composites was made through FESEM, as shown in Figure 7, for the composite containing 25 wt % of the filler.
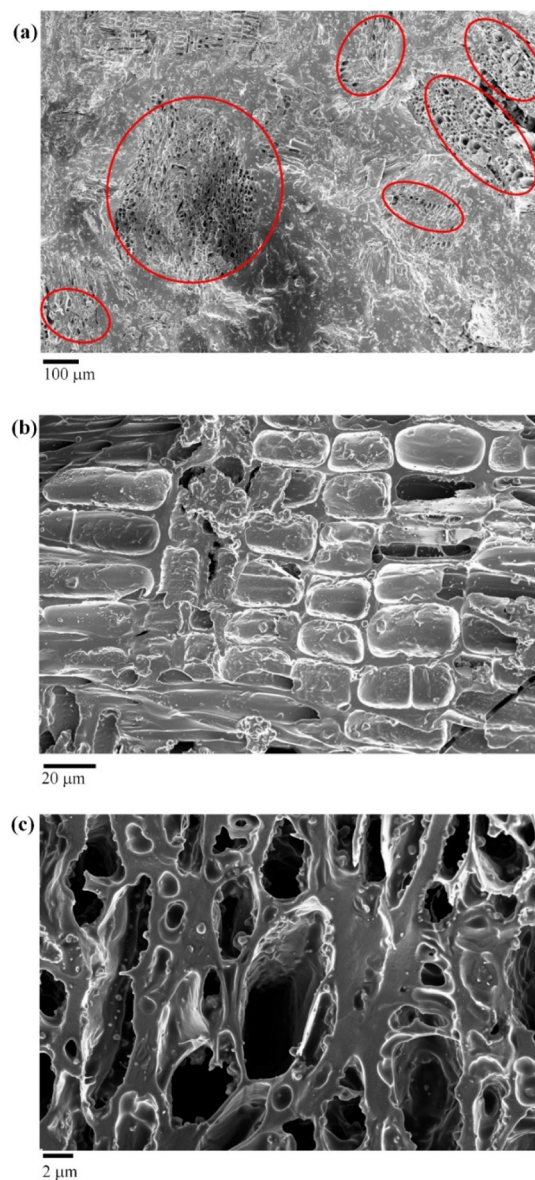

Figure 7. FESEM captions at different magnifications of sections of TAOB-based composites produced by using 25 wt % of the filler. (a) Overview of the composite section and (b,c) two spots of the biochar inclusions.

As clearly evidenced by Figure 7a, big particle clusters were detected, with the particle size ranging from 100 to 200 μm with a good cluster−cluster separation. Silicon interacts well with the TAOB porous structure filling the pores (Figure 7b) through weak interaction and not by chemical bonding. This was proved by observing those areas (Figure 7c) where silicon was removed from the TAOB channel during the FESEM sample preparation.

Composites with a filler percentage ranging from 15 up to 30 wt % were tested under pressure for monitoring their piezoresistive behavior, as shown in Figure 8.
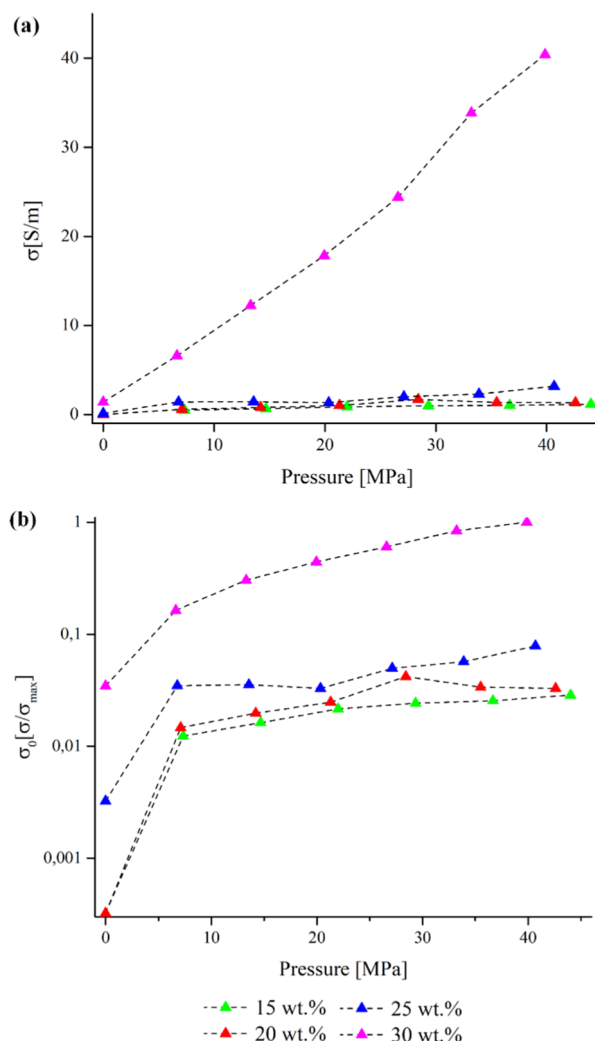

Figure 8. (a) Electrical conductivity measurement as a function of pressure on fillers and related composites containing biochar with a loading ranging from 15 to 30 wt % and (b) electrical conductivity normalized (σ_0) to the highest value measured across the pressure range investigated (σ_{max}).

First, we evaluated the electrical conductivity of the composites under a wide range of applied pressure values. Under compression, the silicon matrix undergoes an elastic deformation that brings filler particles closer, leading to an increase in electrical conductivity. Without applying any stress, composites filled with 15 and 20 wt % showed an insulator behavior, while those filled with 25 and 30 wt % showed conductivities of 0.1 and 1.4 S/m, respectively, measured accordingly with Giorcelli et al.[17] By applying a pressure close to 7 MPa, we observed an increase in conductivity to around 0.5 S/m for the composites filled with 15 and 20 wt %, while those filled with 25 and 30 wt % reached 1.4 and 6.6 S/m, respectively. This pronounced increment is readily appreciable by considering normalized conductivity (σ_0), as shown in Figure 8b. After a first relevant increase, further pressure enhancements induce smaller increments, although larger for higher filler percentages. The composite containing 30 wt % of

TAOB reached a conductivity of 40.0 S/m at 40 MPa, while the one containing 25 wt % of TAOB reached only 3.2 S/m. The other sample conductivity value was close to 1.1 S/m. Even if the composite containing 30 wt % of TAOB achieved better performances, it failed from a mechanical point of view because the high filler percentage weakened the composite structure excessively. After the pressure was released, the composite containing 30 wt % of TAOB showed several macroscopic cracks in all its structure, while the other materials did not crack. Accordingly, for the application, we singled out the composite containing 25 wt % of TAOB that represented the best compromise between the electrical conductivity behavior and mechanical properties with a well-dispersed particle cluster, as shown in Figure 7a. Therefore, we estimated from the model the minimum traveled path through the 25 wt % composite achieving the results shown in Figure 9.
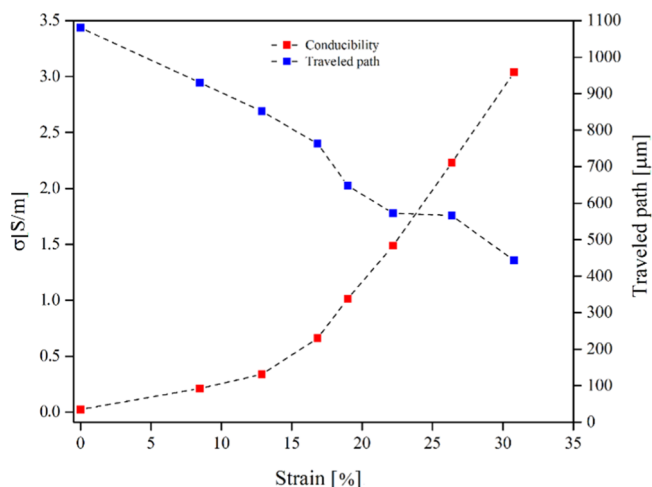

Figure 9. Conductivity and traveled path vs the strain of TAOB-based composites produced by using 25 wt % of the filler.

By randomly dispersing 700 particles having a particle distribution similar to the measured one (Figure 5) in the computed volume, we were able to simulate a composite with a filler loading of around 25 wt %. As reported in Figure 8, as the compressive strain increases, the traveled path decreased from 1080 down to 443 μm and the electrical conductivity rose from 0.1 up to 3.2 S/m. This is consistent with the decrease in the average distance among TAOB particles and to the fact that some TAOB particles will come in contact as compressive strain is increased.

3.3. Device Characterization. The conductivity of the biochar composite key unit was measured by using different composite thicknesses, as shown in Figure 10.

Data observed for the 8 mm thick BCEC were in good agreement with those observed before for the neat composites with the same filler percentage reaching a conductivity close to 3 S/m. On its side, 4 mm thick BCEC reached a higher conductivity at high pressure close to 120 S/m. Based on the traveled path modeling, we assumed that this was due to the higher strain that leads to a system where the particles were closer for thinner BCEC with a lower traveled path and higher electrical conductivity values. Additionally, we tested the reversibility of the system and we observed that the thicker biochar composite key showed a perfect reversibility upon three cycles, while the 8 mm biochar composite key showed a partial detachment of one electrode from the composite,
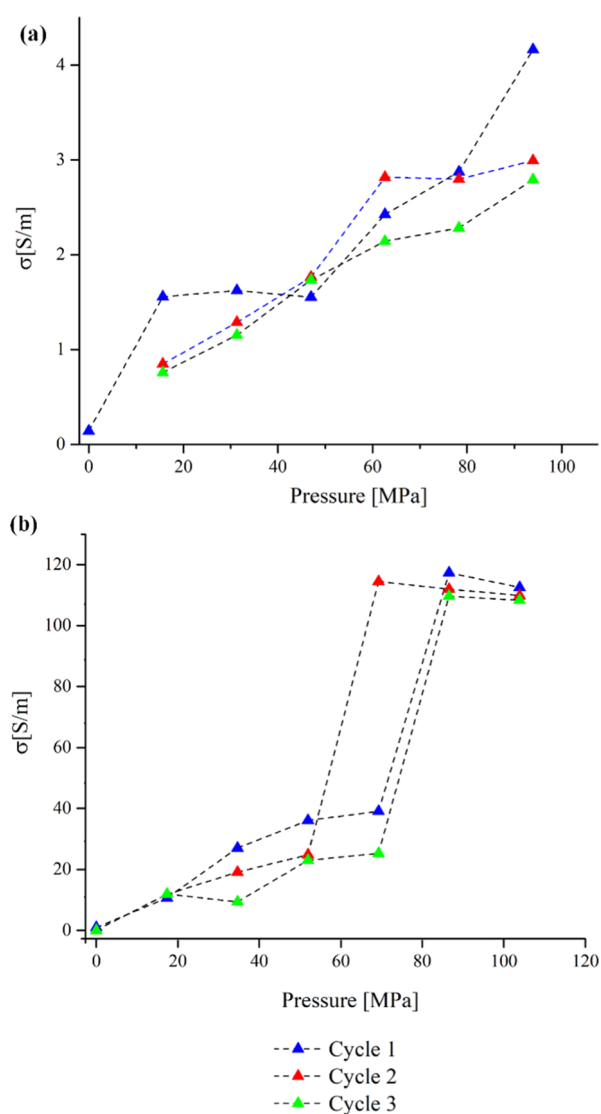
Figure 10. Conductivity vs pressure trends of the 25 wt % BCEC with two different thicknesses of (a) 8 and (b) 4 mm during three consecutive compressive cycles.

altering the noncompressive strain value. Finally, we used the biochar composite keys with the designed demonstration board to show one of the different applications we can achieve with our work. The indicator LED correctly changed colors proportionally to the force applied on the biochar composite indicating, as a proof-of-concept, that it can perform the next engineering step toward the market. The Supporting Information video is available to see the device-operating principle.

4. CONCLUSIONS

We reported for the first time the use of thermally annealed biochar for the production of a fully reversible silicon-rubber piezoresistive material. TAOB reached a remarkable electrical conductivity of up to 10^3 S/m with a highly ordered structure compared with its precursor as shown by Raman analysis. The TAOB-based composites were tested for evaluating their piezoresistive behavior, and an optimum filler concentration of 25 wt % was used for the assembling of a real and functional electronic device based on biochar. To the best of our knowledge, it is the first document of the preparation of an electronic device based on the biochar-containing silicon composite. We hope that will lead the way for a new wave of advanced materials oriented to sustainability.

■ ASSOCIATED CONTENT

ⓢ Supporting Information

The Supporting Information is available free of charge at https://pubs.acs.org/doi/10.1021/acsaelm.0c00971.

Device demonstration video (MP4)

■ AUTHOR INFORMATION

Corresponding Author

Mauro Giorcelli − *Department of Applied Science and Technology, Politecnico di Torino, Turin 10129, Italy; Center for Sustainable Future Technologies, Istituto Italiano di Tecnologia, Torino 10129, Italy;* ⓞ orcid.org/0000-0002-9620-2357; Phone: +39011094326; Email: mauro.giorcelli@polito.it

Authors

Mattia Bartoli − *Department of Applied Science and Technology, Politecnico di Torino, Turin 10129, Italy;* ⓞ orcid.org/0000-0002-4678-0212

Alessandro Sanginario − *Department of Electronics and Telecommunications, Politecnico di Torino, Torino 10129, Italy*

Elisa Padovano − *Department of Applied Science and Technology, Politecnico di Torino, Turin 10129, Italy*

Carlo Rosso − *Department of Mechanical and Aerospace Engineering, Politecnico di Torino, Torino 10129, Italy*

Massimo Rovere − *Department of Applied Science and Technology, Politecnico di Torino, Turin 10129, Italy*

Alberto Tagliaferro − *Department of Applied Science and Technology, Politecnico di Torino, Turin 10129, Italy; Faculty of Science, Ontario Tech University, Oshawa L1H 7K4, Canada*

Complete contact information is available at:
https://pubs.acs.org/10.1021/acsaelm.0c00971

Author Contributions

The manuscript was written through contributions of all authors. All authors have given approval to the final version of the manuscript.

Notes

The authors declare no competing financial interest.

■ ACKNOWLEDGMENTS

■ REFERENCES

(1) Sohi, S. P.; Krull, E.; Lopez-Capel, E.; Bol, R. A review of biochar and its use and function in soil. *Advances in Agronomy*; Elsevier, 2010; pp 47−82.

(2) Cha, J. S.; Park, S. H.; Jung, S.-C.; Ryu, C.; Jeon, J.-K.; Shin, M.-C.; Park, Y.-K. Production and utilization of biochar: A review. *J. Ind. Eng. Chem.* **2016**, *40*, 1−15.

(3) Bartoli, M.; Giorcelli, M.; Jagdale, P.; Rovere, M.; Tagliaferro, A. A Review of Non-Soil Biochar Applications. *Materials* **2020**, *13*, 261.

(4) Das, O.; Sarmah, A. K.; Bhattacharyya, D. Structure−mechanics property relationship of waste derived biochars. *Sci. Total Environ.* **2015**, *538*, 611−620.

(5) Das, O.; Sarmah, A. K.; Bhattacharyya, D. A sustainable and resilient approach through biochar addition in wood polymer composites. *Sci. Total Environ.* **2015**, *512−513*, 326−336.

(6) Arrigo, R.; Bartoli, M.; Malucelli, G. Poly (lactic Acid)−Biochar Biocomposites: Effect of Processing and Filler Content on Rheological, Thermal, and Mechanical Properties. *Polymers* **2020**, *12*, 892.

(7) Bartoli, M.; Rosso, C.; Giorcelli, M.; Rovere, M.; Jagdale, P.; Tagliaferro, A.; Chae, M.; Bressler, D. C. Effect of incorporation of microstructured carbonized cellulose on surface and mechanical properties of epoxy composites. *J. Appl. Polym. Sci.* **2020**, *137*, 48896.

(8) Bartoli, M.; Giorcelli, M.; Rosso, C.; Rovere, M.; Jagdale, P.; Tagliaferro, A. Influence of Commercial Biochar Fillers on Brittleness/Ductility of Epoxy Resin Composites. *Appl. Sci.* **2019**, *9*, 3109.

(9) Arrigo, R.; Jagdale, P.; Bartoli, M.; Tagliaferro, A.; Malucelli, G. Structure−Property Relationships in Polyethylene-Based Composites Filled with Biochar Derived from Waste Coffee Grounds. *Polymers* **2019**, *11*, 1336.

(10) Zhang, Q.; Yi, W.; Li, Z.; Wang, L.; Cai, H. Mechanical properties of rice husk biochar reinforced high density polyethylene composites. *Polymers* **2018**, *10*, 286.

(11) Peterson, S. C.; Kim, S. Reducing Biochar Particle Size with Nanosilica and Its Effect on Rubber Composite Reinforcement. *J. Polym. Environ.* **2020**, *28*, 317−322.

(12) Khan, A.; Savi, P.; Quaranta, S.; Rovere, M.; Giorcelli, M.; Tagliaferro, A.; Rosso, C.; Jia, C. Low-cost carbon fillers to improve mechanical properties and conductivity of epoxy composites. *Polymers* **2017**, *9*, 642.

(13) Khan, A.; Jagdale, P.; Rovere, M.; Nogués, M.; Rosso, C.; Tagliaferro, A. Carbon from waste source: An eco-friendly way for strengthening polymer composites. *Composites, Part B* **2018**, *132*, 87−96.

(14) Li, S.; Harris, S.; Anandhi, A.; Chen, G. Predicting biochar properties and functions based on feedstock and pyrolysis temperature: A review and data syntheses. *J. Cleaner Prod.* **2019**, *215*, 890−902.

(15) Tomczyk, A.; Sokołowska, Z.; Boguta, P. Biochar physicochemical properties: pyrolysis temperature and feedstock kind effects. *Rev. Environ. Sci. Bio/Technol.* **2020**, *19*, 191−215.

(16) Noori, A.; Bartoli, M.; Frache, A.; Piatti, E.; Giorcelli, M.; Tagliaferro, A. Development of Pressure-Responsive PolyPropylene and Biochar-Based Materials. *Micromachines* **2020**, *11*, 339.

(17) Giorcelli, M.; Bartoli, M. Development of Coffee Biochar Filler for the Production of Electrical Conductive Reinforced Plastic. *Polymers* **2019**, *11*, 1916.

(18) Bartoli, M.; Nasir, M. A.; Passaglia, E.; Spiniello, R.; Jagdale, P.; Rosso, C.; Giorcelli, M.; Rovere, M.; Tagliaferro, A. Influence of pyrolytic thermal history on olive pruning biochar and related epoxy composites mechanical properties. *J. Compos. Mater.* **2019**, *54*, 002199831988873.

(19) Bartoli, M.; Giorcelli, M.; Rovere, M.; Jagdale, P.; Tagliaferro, A.; Chae, M.; Bressler, D. C. Shape tunability of carbonized cellulose nanocrystals. *SN Appl. Sci.* **2019**, *1*, 1661−1676.

(20) Giorcelli, M.; Savi, P.; Khan, A.; Tagliaferro, A. Analysis of biochar with different pyrolysis temperatures used as filler in epoxy resin composites. *Biomass Bioenergy* **2019**, *122*, 466−471.

(21) Giorcelli, M.; Khan, A.; Pugno, N. M.; Rosso, C.; Tagliaferro, A. Biochar as a cheap and environmental friendly filler able to improve polymer mechanical properties. *Biomass Bioenergy* **2019**, *120*, 219−223.

(22) Savi, P.; Yasir, M.; Bartoli, M.; Giorcelli, M.; Longo, M. Electrical and Microwave Characterization of Thermal Annealed Sewage Sludge Derived Biochar Composites. *Appl. Sci.* **2020**, *10*, 1334−1345.

(23) Eom, Y.; Son, S. M.; Kim, Y. E.; Lee, J.-E.; Hwang, S.-H.; Chae, H. G. Structure evolution mechanism of highly ordered graphite during carbonization of cellulose nanocrystals. *Carbon* **2019**, *150*, 142−152.

(24) Downie, A.; Crosky, A.; Munroe, P. Physical properties of biochar. *Biochar for Environmental Management: Science and Technology*; Earthscan, 2009, Vol. *1*.

(25) Chen, L.; Chen, G. H.; Lu, L. Piezoresistive behavior study on finger-sensing silicone rubber/graphite nanosheet nanocomposites. *Adv. Funct. Mater.* **2007**, *17*, 898−904.

(26) Nan, N.; DeVallance, D. B. Development of poly (vinyl alcohol)/wood-derived biochar composites for use in pressure sensor applications. *J. Mater. Sci.* **2017**, *52*, 8247−8257.

(27) Shit, S. C.; Shah, P. A review on silicone rubber. *Natl. Acad. Sci. Lett.* **2013**, *36*, 355−365.

(28) Strongone, V.; Bartoli, M.; Jagdale, P.; Arrigo, R.; Tagliaferro, A.; Malucelli, G. Preparation and Characterization of UV-LED Curable Acrylic Films Containing Biochar and/or Multiwalled Carbon Nanotubes: Effect of the Filler Loading on the Rheological, Thermal and Optical Properties. *Polymers* **2020**, *12*, 796.

(29) Barbalini, M.; Bartoli, M.; Tagliaferro, A.; Malucelli, G. Phytic Acid and Biochar: An Effective All Bio-Sourced Flame Retardant Formulation for Cotton Fabrics. *Polymers* **2020**, *12*, 811.

(30) Gabhi, R. S.; Kirk, D. W.; Jia, C. Q. Preliminary investigation of electrical conductivity of monolithic biochar. *Carbon* **2017**, *116*, 435−442.

(31) Castellino, M.; Rovere, M.; Shahzad, M. I.; Tagliaferro, A. Conductivity in carbon nanotube polymer composites: A comparison between model and experiment. *Composites, Part A* **2016**, *87*, 237−242.

(32) Dijkstra, E. W. A note on two problems in connexion with graphs. *Numer. Math.* **1959**, *1*, 269−271.

(33) Jing, X.; Zhao, W.; Lan, L. The effect of particle size on electric conducting percolation threshold in polymer/conducting particle composites. *J. Mater. Sci. Lett.* **2000**, *19*, 377−379.

(34) Ferrari, A. C.; Robertson, J. Interpretation of Raman spectra of disordered and amorphous carbon. *Phys. Rev. B: Condens. Matter Mater. Phys.* **2000**, *61*, 14095.

(35) Dasgupta, D.; Demichelis, F.; Tagliaferro, A. Electrical conductivity of amorphous carbon and amorphous hydrogenated carbon. *Philos. Mag. B* **1991**, *63*, 1255−1266.

(36) Gutiérrez-Pardo, A.; Ramírez-Rico, J.; Cabezas-Rodríguez, R.; Martínez-Fernández, J. Effect of catalytic graphitization on the electrochemical behavior of wood derived carbons for use in supercapacitors. *J. Power Sources* **2015**, *278*, 18−26.